Applied Radiation and Isotopes 191 (2023) 110553

Contents lists available at ScienceDirect

Applied Radiation and Isotopes

journal homepage: www.elsevier.com/locate/apradiso

Evaluation of F-18 FDG radiopharmaceuticals through Molecular Docking and radiation effects

Ozge Kilicoglu [a,b,*], Nayim Sepay [c], Emre Ozgenc [d], Evren Gundogdu [d], Umit Kara [e], Sultan Alomairy [f], M.S. Al-Buriahi [g]

[a] Vocational School of Health Services, Marmara University, Kartal, Istanbul, Turkey
[b] Radiation Laboratory, University of Notre Dame, Notre Dame, IN, 46556-5670, USA
[c] The Department of Chemistry, Lady Brabourne College, India
[d] The Department of Radiopharmacy, Faculty of Pharmacy, Ege University, Bornova, Izmir, Turkey
[e] The Vocational School of Health Services, Medical Imaging Department, Suleyman Demirel University, Isparta, Turkey
[f] Department of Physics, College of Science, Taif University, P.O.Box 11099, Taif, 21944, Saudi Arabia
[g] Department of Physics, Sakarya University, Sakarya, Turkey

ARTICLE INFO

Keywords:
FDG
Docking
MAC
Z_{eff}
MSP
PR

ABSTRACT

Fluorodeoxyglucose (FDG), marked with the most used Positron Emission Tomography (PET) radiopharmaceutical Fluorine-18 (F-18), is a glucose analog and is taken to living cells through membrane glucose carriers. F-18 FDG involvement in tissue is proportional to glucose use. In many cancers, there is increased glucose use due to increased gluten expression and hexokinase activity. F-18 FDG PET is a proven method for diagnosis, staging, re-staging, and evaluation of treatment response in oncology. The purpose of this study is to find the effect of ionizing radiation on proteins in the mechanism of action of FDG and determine to Molecular mechanisms of F-18 FDG accumulation in metabolism. In the study, two different models were used together, the first method, the study was Molecular Docking method for modeling molecules deconstructed and the structure of FDG was energy minimized by utilizing the density functional theory, and the B3LYP functional was used with 6-311G basis set. The second method was the Monte Carlo method for modeling ionizing radiation interactive with the potential routes of FDG metabolism within the cell. It was determined that the Gibbs free energy (ΔG) change was compatible with the ionizing radiation factors for binding of FDG to the aphthous regions of Glucose-6-phosphate isomerase (G1), hexokinase (G2), and glucose transporter-1 (G3) were selected. In this study, the strong binding of FDG to protein influences the effect of radiation on the active site of enzymes. The G1 and G3 shown in the study interacted with only one charged amino acid FDG, and the absence of an aromatic residue around it can be considered among the results of this study as the cause of the low protective effect against ionizing radiation.

1. Introduction

Radiopharmaceuticals are used in diagnostic or therapeutic applications that help to evaluate the clinical translation of diseases especially different types of cancer. They contain pharmaceutical and radioactive parts. The design of radiopharmaceuticals requires upfront decisions regarding combining a suitable pharmaceutical part with an appropriate radionuclide, considering the type and location of the molecular target, the desired application, and the time constraints imposed by the relatively short half-life of the radionuclides (Vermeulen et al., 2019).

Positron emission tomography (PET) is one of the most rapidly growing areas in nuclear imaging and PET radiopharmaceuticals have an important role in the clinical management of cancer patients. Among PET radiopharmaceuticals, F-18 is the most used radionuclide in the preparation of PET radiopharmaceuticals. It decays to 97% positron emission (β+) and has a half-life of 109.7 min and positron energy of 635 keV (Jacobson et al. 2015).

The β+ emitted by the F-18 radionuclide is ionizing radiation. Ionizing radiation has the energy to remove electrons from the orbits of the atoms it affects. Ionizing radiations occur in two forms (wave or particle). The positron is ionizing radiation in a wave structure. The positron has the same mass as the electron but is positively charged and is the electron's antiparticle. Unstable nuclei perform electron capture

* Corresponding author. Vocational School of Health Services, Marmara University, Kartal, Istanbul, Turkey.
E-mail address: ozgekoglu@gmail.com (O. Kilicoglu).

https://doi.org/10.1016/j.apradiso.2022.110553
Received 25 July 2022; Received in revised form 23 October 2022; Accepted 2 November 2022
Available online 5 November 2022
0969-8043/© 2022 Elsevier Ltd. All rights reserved.

or positron emission to get rid of excess protons. In positron emission, a proton turns into a neutron and a positively charged electron and neutrino are formed. The resulting positron collides with an electron, resulting in an annihilation reaction and two gamma rays are formed in the environment. The energy of each beam is 511 keV and they move in the opposite direction with an angle of 180°. In PET camera systems, to detect photons going in the opposite direction, the detectors are placed opposite each other, and images are taken (Muehllehner and Karp 2006).

F-18 FDG is a common administration PET radiopharmaceutical and is prepared by using F-18. It localizes tumors, monitors response to treatment, and determines prognosis in patients with various cancers. The pharmaceutical part of F-18 FDG forms from FDG. FDG is a glucose analog and PET is used to assess metabolic activity by measuring FDG accumulation (de Geus-Oei et al., 2009). FDG participates in glucose metabolism and its uptake mechanism is formed from facilitated diffusion via glucose transporters. Glucose is phosphorylated by the enzyme hexokinase (HXK) to glucose 6-phosphate, which subsequently is metabolized to carbon dioxide and water in the cytosol during the uptake mechanism process. Deoxy glucose (DG) enters the cell similarly to glucose and is converted to deoxyglucose 6-phosphate which, however, does not undergo further metabolism and is trapped in the cancer cells. As a glucose analog, FDG enters the cell membrane using the same transporters as glucose. It is then phosphorylated into [18F]-FDG-6-phosphate. This metabolite is not a substrate for further enzymes and thus is trapped and accumulates inside the cell in proportion to the metabolism of glucose (Buchanan 2017; Shiue and Welch 2004).

Most cancer cells tend to metabolize glucose by glycolysis in the presence of oxygen, which is increased compared to normal cells. This increased glucose metabolism leads to the accumulation of F-18 FDG in cancer cells, which results in positive signals on Fluorodeoxyglucose-Positron Emission Tomography/Computed Tomography (FDG-PET/CT) scans, providing information about the disease. However, the mechanisms by which F-18 FDG accumulates in cancer tissues are complex (Gillies et al. 2008). F-18 FDG does not specifically accumulate in cancer cells; it may also accumulate in inflamed areas where glucose utilization is increased. Despite its clinical utility, the cellular and molecular mechanisms of F-18 FDG accumulation have not yet been elucidated (Plathow and Weber 2008). F-18 FDG enters the cell via the glucose transporter (GLUT) family of 14 promoters and is then phosphorylated by HXKs to FDG-6 phosphate, which is stored in the cell due to its negatively charged state. The increase in GLUT receptors usually occurs in the presence of cancer cells and is associated with poor prognosis in patients. Although different tumor types express different GLUT receptors at different levels, upregulation of the GLUT1 receptor is common in most cancers and is associated with tumor stage and prognosis (Kawada et al. 2016). In addition to this condition, increased levels of HXK are seen in many cancers. HXK binds to the mitochondrial membrane and efficiently phosphorylates FDG to FDG-6 phosphate. As a result of this phosphorylation, FDG cannot be passed from the cell to another location and accumulates in the cell. Phosphorylated FDG can be dephosphorylated with glucose-6-phosphatase to F-18 FDG, but dephosphorylation is slow. Dephosphorylation of the phosphorylated polar presence of FDG occurs relatively slowly in cancer cells, which generally lack glucose-6-phosphatase or have low levels of glucose-6-phosphatase compared with noncancerous cells. The cellular concentration of F-18 FDG indicates the accumulation of F-18 FDG and the glycolytic activity of exogenous glucose. From the amount of FDG accumulated in tissue over a period, the rate of glucose uptake by that tissue can be calculated. Accumulation of F-18 FDG is strongly dependent on GLUT1 and the rate-limiting glycolytic enzyme HXK in most cancers (Medina and Owen 2002; Jadvar et al. 2009; Smith 1999; Mathupala, Ko, and and Pedersen 2006; Smith 2000).

It is known that three main factors affect the accumulation of FDG in cancer cells. FDG is transported into the cell by glucose transport proteins such as GLUT1. When transported into the cell, FDG is phosphorylated by the glycolytic enzyme hexokinase to become F-18 FDG-phosphate, which accumulates within the tumor cell due to the low membrane permeability of FDG-6-phosphate. The levels of FDG-PO4 also depend on the activity of glucose-6-phosphatase, the enzyme which removes the phosphate from this compound (Burt et al., 2001). Hence, high levels of glucose-6-phosphatase accelerate the conversion of FDG-6-phosphate to FDG, reducing the accumulation of FDG and causing its release from cells (Izuishi et al., 2014). The low radiation effect of glucose-6-phosphatase reduces the conversion of FDG-6-phosphate to FDG and increases the retention of FDG in the target site.

The use of the radiopharmaceutical F-18 FDG in oncology is based on the rate difference in glucose metabolism and glucose uptake rate in benign and malignant cells. In addition, F-18 FDG uptake is also accelerated in inflammatory processes such as infections, granulomas, and other processes, leading to false positives and lower specificity. The uptake of F-18 FDG can vary widely in different tumor types. The observation of high uptake in the PET image following FDG uptake is generally associated with a high number of viable tumor cells, high GLUT1 expression, and an increase in hexokinase enzyme activity.

In this article, docking studies are used to examine the mechanism of action of FDG and the effect of its radiation on binding proteins. Glucose-6-phosphate isomerase (G1), hexokinase (G2), and glucose transporter-1 (G3) proteins were selected for this study. The ionizing radiation interaction of the G1, G2, and G3 can be understood through various parameters expressing the ability of the proteins to attenuate/absorb radiation.

2. Material and method

2.1. Docking study

The structure of FDG was energy minimized by utilizing the density functional theory. The B3LYP functional was used with a 6-311G basis set. This structure has been utilized for docking. The protein structure of G1, HXK, and GLUT1 used for the calculations were downloaded from the RCSB website and the protein data bank (PDB) codes are 1HM5, 1QHA, and 5EQH respectively (Cordeiro et al., 2003; Rosano et al., 1999; Kapoor et al., 2016). The structure preparation of the proteins has been performed by Molecular Graphics Laboratory (MGL) Tools. Auto Dock 4.2 was utilized for all the calculations and the Lamarckian algorithm was employed (Sousa et al. 2006). An 80 x 80 x 80 grid box was used for docking calculations. Discovery Studio 2017 R2 client and Samson 2020 R2 were utilized for visualization and structural analysis of the docking results.

2.2. Monte Carlo simulations and nuclear radiation attenuation properties

Ionizing radiation interaction with matter can be understood via several parameters that express the ability of matter to attenuate/absorb the radiation. For photon interaction (e.g. x and gamma rays interaction), the mass attenuation coefficient (MAC) is a very important quantity that helps to differentiate the photon attenuation capacity of the matter (Berger 2005; Sharifi et al. 2013). The MAC values play the main role to determine vital related parameters, such as effective atomic number (Z_{eff}), for photon attenuation characterization (Ozge Kilicoglu et al., 2022b; Vahapoglu et al., 2022; Ozdogan et al., 2022).

In the current investigation, both the WinXCOM program and MATLAB simulation were employed to evaluate the MAC values for [18F]-FDG interaction with enzymes such as D-Glucose 6-phosphate isomerase, Hexokinase, and protein such as Glucose transporter 1.

The theoretical base of MAC calculation depends on Beer-Lambert law as $\varphi_t(E, x_m) = \varphi_o(E)e^{-MAC\ x_m}$. Here, φ_o is incident photons flux, x_m is the mass thickness, and φ_t is the transmitted flux through the matter.

For the charged particle interaction (heavy charged particles such as proton and alpha), the mass stopping powers (MSP) and projectile (incident particle) range are very important quantities that help to differentiate the proton/alpha attenuation capacity of matter. In the current investigation, we used the SRIM platform for determining both MSP and ranges for the heavy charged particles(J. F. Ziegler 2004; J. Ziegler et al. 2008)

3. Results and discussions

3.1. Docking study

The interaction of synthetic and natural products with bio-macro molecules can be understood through docking study (Sepay et al., 2016, 2017). To find the mechanism of action of FDG and the effect of its radiation on the binding proteins, docking studies have been utilized. In this case, G1, HXK (G2) and GLUT1 (G3) have been chosen for the study. The docking results showed that the FDG molecules can bind with all these samples at their active site. However, the binding affinity of FDG with these proteins are non-identical. The change of Gibbs free energy (ΔG) for the binding of the fluorinated glucose at the active site of the glucose-6-phosphate isomerase, HXK, and GLUT1 are -12.89 kcal/mol, -14.11 kcal/mol, and -10.37 kcal/mol respectively. Therefore, the strong protein bind of FDG can influence their radiation effect of them.

To understand how the radiation effect occurs, a deep structural investigation is required. The binding of the FDG at the active site of the G2 is shown in Fig. 1a. The molecule gets an amphiphilic environment inside this pocket (Fig. 1 b). In this site, the molecule interacts with F67, V68, R69, S70, and V456 amino acid residues (Fig. 1 c) through hydrogen bond (green) and C–H … π interactions (faint green). The electromagnetic radiation of FDG's F atom can interact with the aromatic electrons of F67 and the charge of R69 amino acid residues. Such interactions may play an important role in its high radiation effect. In the case of G1 and G3, only one charged amino acid interacted with the FDG (Fig. 2 (a), (b)) and the absence of aromatic residue in the vicinity of it may be the cause of low protection against ionizing radiation.

Therefore, the strong binding of FDG at the active site of a protein can reduce the effect of radiation energy on the protein through efficient energy transfer to the nearest aromatic and charged amino acid residues, and thus the protein exhibits a high protective effect.

3.2. Nuclear radiation attenuation properties

Shielding, research, and simulation work are extensively used in the literature to examine gamma-ray attenuation parameters in identifying the best material available (Ozge Kilicoglu and Mehmetcik, 2021). The composition of G1, G2 enzymes and G3 protein was given in Table 1. The MAC values of the present enzymes and protein (Glucose 6-phosphate isomerase, HXK, and GLUT1) were obtained via MATLAB simulation, and direct calculations via the WinXCOM platform for the energy spectrum of photons within the range 0.015–2 MeV are listed in Table 2. To compare MAC values obtained via the two procedures, the factor namely Dev. (in %) is used in this task. This factor was calculated based on the expression:

$$\text{Dev. } (\%) = \left| \left[(\text{MAC})_{\text{WinXCOM}} - ((\text{MAC}))_{\text{MATLAB}} \right] \div ((\text{MAC}))_{\text{WinXCOM}} \right| \times 100 \quad (1)$$

Such factor of Dev. (%) is quantitatively referred to as the deviation in the value of MAC obtained via the two aforementioned procedures at each photon energy. With respect to the listed values of Dev in Table 2, it is clear and safe to conclude that results from the two aforementioned procedures are in agreement and comparable to each other. For all of the studied enzymes and protein (Glucose 6-phosphate isomerase, Hexokinase, and Glucose transporter 1) the maximum value of Dev. (%) was

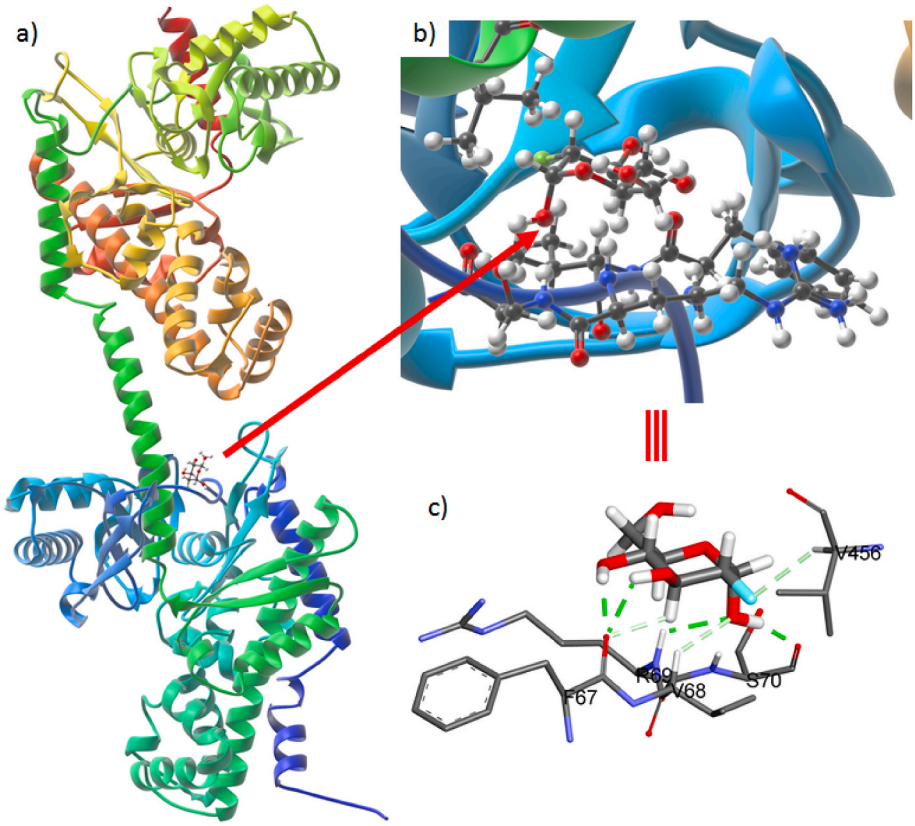

Fig. 1. (a) Docking pose of FDG at the active site of hexokinase, (b) the micro environment of FDG, (c) various non-covalent interactions between FDG and amino acids of hexokinase.

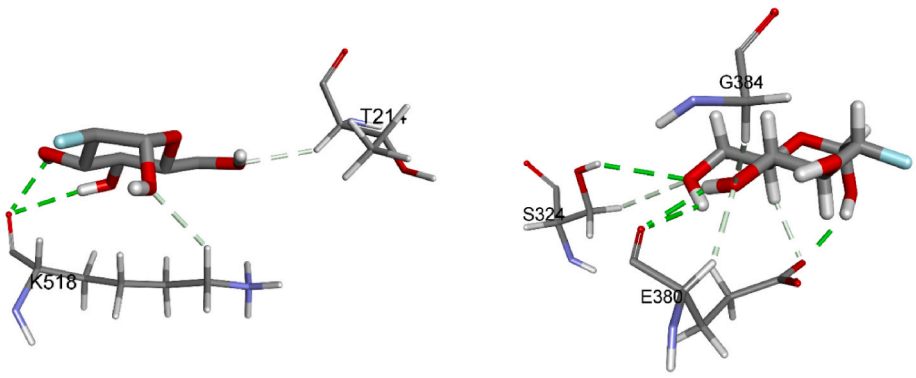

Fig. 2. various non-covalent interactions between FDG and amino acids of (a) glucose-6-phosphate isomerase and (b) glucose transporter-1.

Table 1
D-Glucose 6-phosphate isomerase, Hexokinase enzymes and Glucose transporter 1 protein codes and elemental compositions.

Sample code	Sample	C	N	O	S	H	Density (g/cm3)
G1	**D-Glucose 6-phosphate isomerase**	54.0572	17.1889	20.6797	1.0221	7.0521	1.678 ± 0.1
G2	**Hexokinase**	52.5361	17.2161	21.194	1.9786	7.0752	1.612 ± 0.1
G3	**Glucose transporter 1**	55.53	16.448	19.448	1.3242	7.2499	1.694 ± 0.1

Table 2
The mass attenuation coefficients (cm2/g) values with F-18 FDG interaction from MATLAB and WinXCOM for G1, G2 enzymes and G3 protein.

G1				G2			G3		
MeV	Matlab	WinXcom	% Dev	Matlab	WinXcom	% Dev	Matlab	WinXcom	% Dev
0.001	2738.735	2739.000	0.000	2753.070	2753.000	0.000	2697.787	2698.000	0.000
0.002	905.295	893.600	0.013	871.158	899.300	0.031	900.765	879.400	0.024
0.002	391.561	393.300	0.004	394.370	396.100	0.004	385.146	386.800	0.004
0.003	226.022	231.300	0.023	248.957	250.500	0.006	215.467	208.800	0.032
0.003	135.169	132.400	0.021	147.891	145.000	0.020	136.791	134.000	0.021
0.004	56.284	56.780	0.009	62.189	62.730	0.009	57.138	57.640	0.009
0.005	29.394	29.230	0.006	32.692	32.510	0.006	29.905	29.740	0.006
0.006	17.028	16.940	0.005	19.053	18.930	0.007	17.556	17.260	0.017
0.008	7.077	7.171	0.013	7.959	8.064	0.013	7.229	7.325	0.013
0.010	3.723	3.719	0.001	4.196	4.192	0.001	3.807	3.803	0.001
0.020	0.617	0.619	0.002	0.679	0.680	0.003	0.629	0.631	0.002
0.030	0.319	0.316	0.009	0.338	0.334	0.010	0.323	0.320	0.009
0.040	0.239	0.240	0.002	0.247	0.247	0.002	0.244	0.241	0.013
0.050	0.209	0.209	0.001	0.213	0.213	0.001	0.210	0.210	0.001
0.060	0.193	0.193	0.002	0.195	0.195	0.002	0.194	0.193	0.002
0.080	0.174	0.174	0.002	0.175	0.175	0.001	0.175	0.175	0.001
0.100	0.163	0.163	0.000	0.164	0.164	0.001	0.163	0.163	0.000
0.200	0.132	0.132	0.001	0.132	0.132	0.001	0.132	0.132	0.000
0.300	0.114	0.114	0.003	0.114	0.114	0.003	0.114	0.114	0.004
0.400	0.102	0.102	0.001	0.102	0.102	0.001	0.102	0.102	0.001
0.500	0.093	0.093	0.002	0.093	0.093	0.001	0.094	0.093	0.001
0.600	0.086	0.086	0.003	0.086	0.086	0.003	0.086	0.086	0.006
0.800	0.076	0.076	0.002	0.076	0.076	0.001	0.076	0.076	0.001
1.000	0.068	0.068	0.000	0.068	0.068	0.000	0.068	0.068	0.000
1.500	0.056	0.055	0.005	0.055	0.055	0.016	0.056	0.056	0.005
2.000	0.048	0.048	0.000	0.048	0.048	0.001	0.048	0.048	0.000

less than 0.05%. This signifies that the simulation outcomes are reliable and accurate.

We plotted MAC values against photon energy for all the G1, G2 enzymes, and G3 protein specimens to appreciate the variation of MAC not only with respect to energy but also with respect to density and chemical composition (Kılıçoğlu, 2019b; Kilicoglu et al., 2021). Fig. 3 represents the MAC profile of the G1, G2 enzymes and G3 protein for incident energy reaching 2 MeV. Clearly, the max. MAC value can be seen at the energy of 0.001 MeV, thereafter there is a remarkable drop in the values of MAC up to 0.002 MeV. Above 0.002 MeV, the MAC values seem to be constant and there is no observable change in MAC with increasing the energy. The trend of MAC for the G1, G2 enzymes, and G3 protein at the considered energy range can be explained based on the photon partial mechanisms. For example, the remarkable drop in MAC values occurred due to the photoelectric absorption, while the multiple interactions produced by Compton scattering led to pausing the variation of MAC values with energy. The Z_{eff} is a quantity that clarifies the effects of atomic numbers of the constituents/elements of a chemical composite material on its photon interaction and absorption ability (Ozge Kilicoglu and Tekin, 2020a; Kara et al., 2020; O. Kilicoglu et al.,

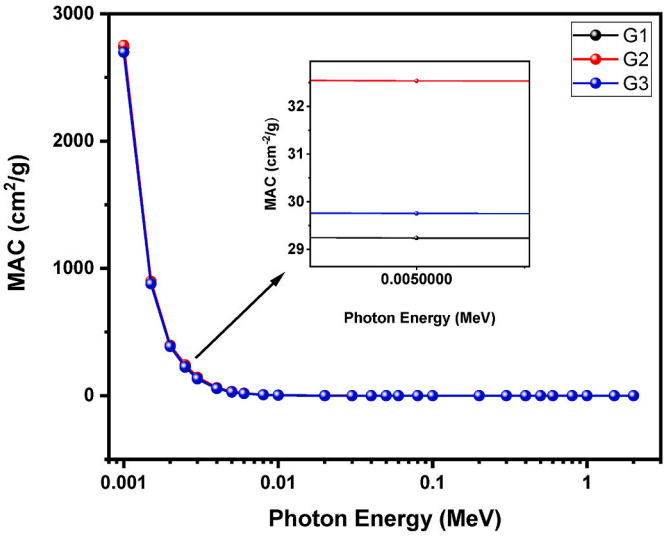

Fig. 3. Variation of mass attenuation coefficient (μ_m) values as a function of photon energy for G1, G2 enzymes and G3 protein.

2022a). Fig. 4 represents the Z_{eff} profile of the G1, G2 enzymes, and G3 protein for incident energy reaching 2 MeV (Kilicoglu, 2019a). Here, one can see that the highest value is around 8 for the specimen of G2 (Hexokinase). The reason for such interesting observation is that the Hexokinase specimen contains the highest content of S element among the studied specimens. Therefore, the photon makes more collisions in this case (e.g., the photon passes through more electrons) leading to more attenuation in the final state of the transmitted photon.

As a second step, we shall discuss the attenuation of heavily charged partials as they pass through the G1, G2 enzymes, and G3 protein for F-18 FDG at kinetic energy reaching 2 MeV. Fig. 5 represents the MSP profile of the G1, G2 enzymes, and G3 protein for the heavy charged particles (a) proton and (b) alpha particles. From Fig. 5 (a), the proton interaction with the results of the present enzymes and protein appears a peek at the kinetic energy of 0.08 MeV with the value of 0.711 MeV cm^2/mg. Thereafter, there is a continuous decrease with increasing the kinetic energy of the incident charged particle. From Fig. 5 (b), the alpha particle interaction with the results of the present enzymes and protein to appear a peak at the kinetic energy of 0.65 MeV with the value of

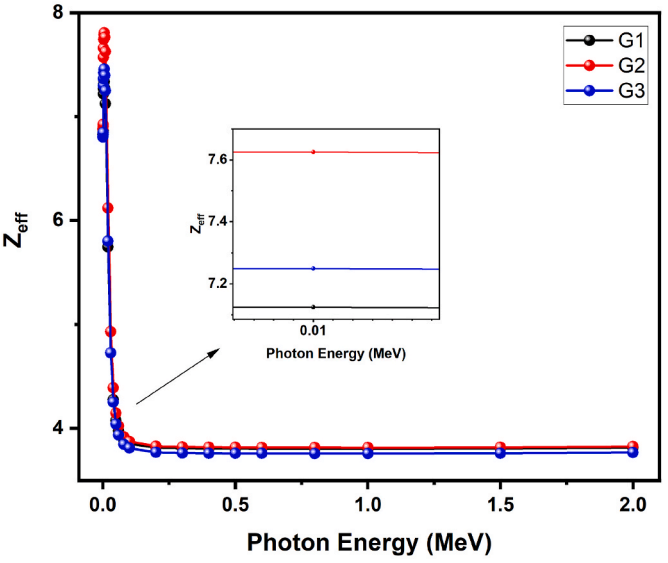

Fig. 4. Variation of effective atomic (Z_{eff}) number values as a function of photon energy for G1, G2 enzymes and G3 protein.

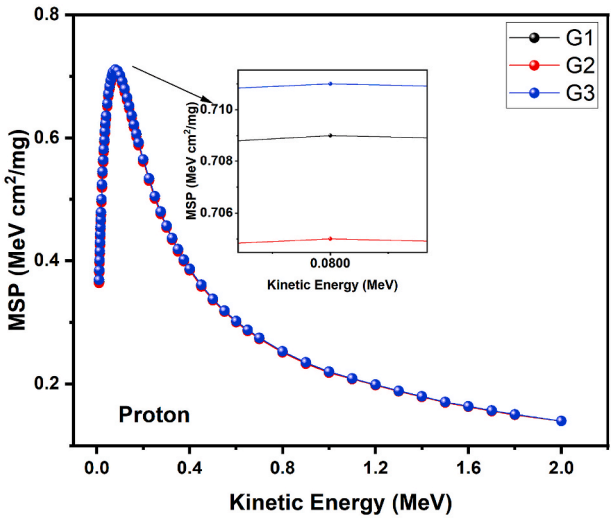

Fig. 5a. Proton mass stopping powers of variation as a function of kinetic energy for the selected G1, G2 enzymes and G3 protein.

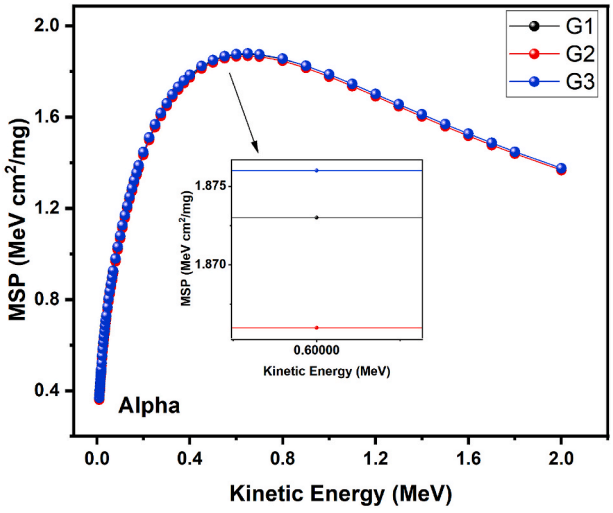

Fig. 5b. Alpha mass stopping powers of variation as a function of kinetic energy for the selected G1, G2 enzymes and G3 protein.

1.879 MeV cm^2/mg. Thereafter, like in the case of the proton, there is a continuous decrease with increasing the kinetic energy of the incident charged particle(Tekin et al., 2020; Alothman et al., 2021; Kilicoglu and Tekin, 2020b). The differences between the proton and alpha interactions with enzymes and protein can be explained based on the projectile mass. Such that, in our study, the mass of the alpha particle is heavier than the mass of the proton. Thus, one needs more power to stop the heavier radiation (alpha in the current work). Fig. 6 represents the projectile range profile of the G1, G2 enzymes, and G3 protein for the heavy charged particles (a) proton and (b) alpha particles. Obviously, the range of G1, G2 enzymes, and G3 protein for proton interaction are higher than that of alpha interaction. This is due to Coulomb's force which is based on the inverse-square law that quantifies the amount of force between two stationaries, electrically charged particles. It is worth mentioning that the specimen of G2 (Hexokinase) possesses the highest values of both MSP and projectile range.

4. Conclusion

In studies conducted to find the effect of ionizing radiation on proteins in the mechanism of action of FDG, it was determined that the ΔG

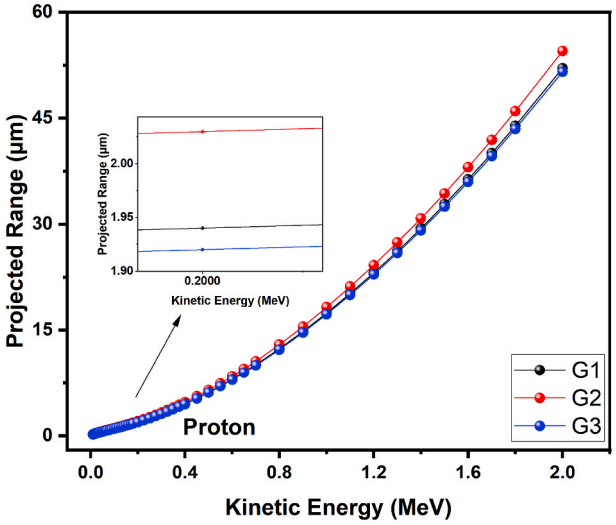

Fig. 6a. Proton projected range as a function of kinetic energy for the selected G1, G2 enzymes and G3 protein.

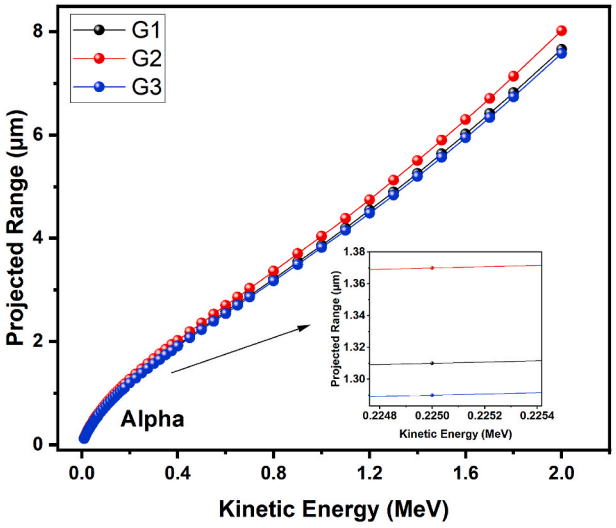

Fig. 6b. Alpha projected range as a function of kinetic energy for the selected G1, G2 enzymes and G3 protein.

change was compatible with the MAC and Z_{eff} values for binding of FDG to the aphthous regions of G1, G2 enzymes, and G3 protein. In this case, the strong binding of FDG to protein affects the effect of radiation on the active site of enzymes. In the G1 enzyme and G3 protein shown in Fig. 2 (a) and (b), only one charged amino acid interacted with FDG, and the absence of an aromatic residue around it could be the reason for the low protective effect against ionizing radiation. The strong binding of FDG in the active site of the enzyme can reduce the effect of radiation energy on the protein through efficient energy transfer to the nearest aromatic and charged amino acid residues so that the protein exhibits a high protective effect. Examination of the FDG metabolic pathway reveals that FDG has a high binding capacity and strong interaction with protein structures in the cell membrane. When these proteins interacting with FDG were examined, it was found that the highest binding capacity belonged to hexokinase. It was interpreted that hexokinase protects the protein structure from radiation thanks to the presence of aromatic and charged amino acid residues in the active site.

It was suggested that the ΔG between G1, G2 enzymes, and G3 protein and FDG is parallel to MAC, Z_{eff}, and that the effect of radiation on these enzymes and protein affects the binding efficiency. It is suggested that the presence of aromatic and charged structures in the binding site protects the protein from the radiation energy and thus increases the binding efficiency. Moreover, these results are consistent with the MAC, Z_{eff}, MSP, and PR values of G1, G2 enzymes and G3 protein. In docking studies, the mechanism of action of FDG and the effect of its radiation on binding proteins with high radiation efficiency were also demonstrated with the ΔG values obtained MAC and Z_{eff} values. The proton and alpha particle protection of FDG was investigated using MSP and PR measurements. Therefore, the MSP values of the enzymes and protein investigated (G2, G1, G3) increased, respectively. As a result, G2 (Hexokinase) was discovered to have the greatest radiation attenuation property.

Understanding the biochemical and pharmaceutical transition pathways related to the disease is critical in designing innovative radiotracers for PET/CT imaging.

This work reveals scientifically how FDG and the substrate of glucose-carrying proteins interact in the cell by attaching itself to the regular glycolytic pathway at the first stage. Furthermore, based on this research, we were able to identify novel PET/CT radiopharmaceuticals with evidence of enhanced GLUT expression and hexokinase activity in a variety of malignancies.

Extensive research in animals and volunteers in simulated settings and in vivo are required for the development of novel radiopharmaceutical formulations. We also think that combining Monte Carlo and Molecular Docking simulation systems in drug discovery and development can lower drug discovery expenses.

CRediT authorship contribution statement

Ozge Kilicoglu: Writing – original draft, Validation, Investigation. **Nayim Sepay:** Investigation. **Emre Ozgenc:** Writing – original draft. **Evren Gundogdu:** Writing – original draft. **Umit Kara:** Investigation. **Sultan Alomairy:** Writing – original draft. **M.S. Al-Buriahi:** Writing – original draft.

Declaration of competing interest

The authors declare that they have no known competing financial interests or personal relationships that could have appeared to influence the work reported in this paper.

Data availability

No data was used for the research described in the article.

Acknowledgment

None.

References

Alothman, Miysoon A., Alrowaili, Z.A., Al-Baradi, Ateyyah M., Kilicoglu, Ozge, Mutuwong, C., Al-Buriahi, M.S., 2021. Elastic properties and radiation shielding ability of ZnO–P2O5/B2O3 glass system. J. Mater. Sci. Mater. Electron. 32 (14), 19203–19217. https://doi.org/10.1007/s10854-021-06442-z.

Berger, Martin J., 2005. XCOM: Photon Cross Section Database (Version 1.3). Http://Physics.Nist.Gov/Xcom.

Buchanan, Elizabeth, 2017. Considering the ethics of big data research: a case of twitter and ISIS/ISIL." edited by sergio gómez. PLoS One 12 (12), e0187155. https://doi.org/10.1371/journal.pone.0187155.

Burt, Bryan M., Humm, John L., Kooby, David A., Squire, Olivia D., Mastorides, Stephen, Larson, Steve M., Fong, Yuman, 2001. Using positron emission tomography with [18F] FDG to predict tumor behavior in experimental colorectal cancer. Neoplasia 3 (3), 189–195.

Cordeiro, A.T., Godoi, P.H.C., Chtp Silva, Garratt, Richard Charles, Oliva, Glaucius, Thiemann, Otávio Henrique, 2003. Crystal structure of human phosphoglucose isomerase and analysis of the initial catalytic steps. Biochim. Biophys. Acta, Proteins Proteomics 1645 (2), 117–122.

Geus-Oei, Lioe-Fee de, Vriens, Dennis, Wm van Laarhoven, Hanneke, van der Graaf, Winette TA., Oyen, Wim JG., 2009. Monitoring and predicting response to

therapy with 18F-FDG PET in colorectal cancer: a systematic review. J. Nucl. Med. 50 (Suppl. 1), 43S–54S.
Gillies, Robert J., Robey, Ian, Gatenby, Robert A., 2008. Causes and consequences of increased glucose metabolism of cancers. J. Nucl. Med. 49 (Suppl. 2), 24S–42S.
Izuishi, Kunihiko, Yamamoto, Yuka, Mori, Hirohito, Kameyama, Riko, Fujihara, Shintaro, Masaki, Tsutomu, Suzuki, Yasuyuki, 2014. Molecular mechanisms of [18F] Fluorodeoxyglucose accumulation in liver cancer. Oncol. Rep. 31 (2), 701–706.
Jacobson, Orit, Kiesewetter, Dale O., Chen, Xiaoyuan, 2015. Fluorine-18 radiochemistry, labeling strategies and synthetic routes. Bioconjugate Chem. 26 (1), 1–18.
Jadvar, Hossein, Alavi, Abass, Gambhir, Sanjiv S., 2009. 18F-FDG uptake in lung, breast, and colon cancers: molecular biology correlates and disease characterization. J. Nucl. Med. 50 (11), 1820–1827.
Kapoor, Khyati, Finer-Moore, Janet S., Pedersen, Bjørn P., Caboni, Laura, Waight, Andrew, Hillig, Roman C., Peter, Bringmann, Heisler, Iring, Müller, Thomas, Holger Siebeneicher, 2016. Mechanism of inhibition of human glucose transporter GLUT1 is conserved between cytochalasin B and phenylalanine amides. In: Proceedings of the National Academy of Sciences, vol. 113, pp. 4711–4716, 17.
Kara, Umit, Kilicoglu, Ozge, Karaibrahimoglu, Adnan, Cavdarli, Kemal, Ince, Fuat, 2020. Radiation attenuation properties of removable partial dentures (RPD). Mater. Chem. Phys. 253 (October), 123301 https://doi.org/10.1016/j.matchemphys.2020.123301.
Kawada, Kenji, Iwamoto, Masayoshi, Sakai, Yoshiharu, 2016. Mechanisms underlying 18F-Fluorodeoxyglucose accumulation in colorectal cancer. World J. Radiol. 8 (11), 880.
Kilicoglu, O., Chaitali, V., More, Akman, F., Dilsiz, K., Oğul, H., Kaçal, M.R., Polat, H., Agar, O., 2022a. Micro Pb filled polymer composites: theoretical, experimental and simulation results for γ-ray shielding performance. Radiat. Phys. Chem. 194, 110039.
Kilicoglu, Ozge, 2019a. Characterization of copper oxide and cobalt oxide substituted bioactive glasses for gamma and neutron shielding applications. Ceram. Int. 45 (17), 23619–23631. https://doi.org/10.1016/j.ceramint.2019.08.073. Part B).
Kilicoglu, Ozge, Kara, Umit, Inanc, Ibrahim, 2021. The impact of polymer additive for N95 masks on gamma-ray attenuation properties. Mater. Chem. Phys. 260 (February), 124093 https://doi.org/10.1016/j.matchemphys.2020.124093.
Kilicoglu, Ozge, Kara, Umit, Ozgenc, Emre, Gundogdu, Evren, 2022b. Pre-clinic study of radiopharmaceutical for covid-19 inactivation: dose distribution with Monte Carlo simulation. Appl. Radiat. Isot. 188, 110364.
Kilicoglu, Ozge, Mehmetcik, Hakan, 2021. Science mapping for radiation shielding research. Radiat. Phys. Chem. 189 (December), 109721 https://doi.org/10.1016/j.radphyschem.2021.109721.
Kilicoglu, Ozge, Tekin, H.O., 2020a. Bioactive glasses and direct effect of increased K2O additive for nuclear shielding performance: a comparative investigation. Ceram. Int. 46 (2), 1323–1333. https://doi.org/10.1016/j.ceramint.2019.09.095.
Kilicoglu, Ozge, Tekin, H.O., 2020b. Bioactive glasses with TiO2 additive: behavior characterization against nuclear radiation and determination of buildup factors. Ceram. Int. 46 (8) https://doi.org/10.1016/j.ceramint.2020.01.088. Part A): 10779–87.
Kılıçoğlu, Özge, 2019b. An investigation on effective atomic numbers and mass attenuation coefficients of some bioactive glasses. European Journal of Science and Technology. https://doi.org/10.31590/ejosat.517731. March, 168–75.
Mathupala, S.P., Ko, Y.H., L, P., Pedersen, 2006. Hexokinase II: cancer's double-edged sword acting as both facilitator and gatekeeper of malignancy when bound to mitochondria. Oncogene 25 (34), 4777–4786.
Medina, Rodolfo A., Owen, Gareth I., 2002. Glucose transporters: expression, regulation and cancer. Biol. Res. 35 (1), 9–26.
Muehllehner, Gerd, Karp, Joel S., 2006. Positron emission tomography. Phys. Med. Biol. 51 (13), R117.
Ozdogan, H., Kilicoglu, O., Akman, F., Agar, O., 2022. Comparison of Monte Carlo simulations and theoretical calculations of nuclear shielding characteristics of various borate glasses including Bi, V, Fe, and Cd. Appl. Radiat. Isot. 189, 110454.
Plathow, Christian, Weber, Wolfgang A., 2008. Tumor cell metabolism imaging. J. Nucl. Med. 49 (Suppl. 2), 43S–63S.
Rosano, Camillo, Sabini, Elisabetta, Rizzi, Menico, Deriu, Daniela, Murshudov, Garib, Bianchi, Marzia, Giordano, Serafini, Magnani, Mauro, Bolognesi, Martino, 1999. Binding of non-catalytic ATP to human hexokinase I highlights the structural components for enzyme–membrane association control. Structure 7 (11), 1427–1437.
Sepay, Nayim, Guha, Chayan, Maity, Sanhita, Asok, K., Mallik, 2017. Synthesis of 6, 12-methanobenzo [d] pyrano [3, 4-g][1, 3] dioxocin-1 (12H)-Ones and study of their interaction with DNA and β-lactoglobulin. Eur. J. Org Chem. 2017 (40), 6013–6022.
Sepay, Nayim, Mallik, Sumitava, Guha, Chayan, Asok, K., Mallik, 2016. An efficient synthesis of 1, 3-dimethyl-5-(2-phenyl-4 H-Chromen-4-Ylidene) pyrimidine-2, 4, 6 (1 H, 3 H, 5 H)-triones and investigation of their interactions with β-lactoglobiulin. RSC Adv. 6 (98), 96016–96024.
Sharifi, Sh, Bagheri, R., Shirmardi, S.P., 2013. Comparison of shielding properties for ordinary, barite, serpentine and steel–magnetite concretes using MCNP-4C code and available experimental results. Ann. Nucl. Energy 53, 529–534.
Shiue, Chyng-Yann, Welch, Michael J., 2004. Update on PET radiopharmaceuticals: life beyond Fluorodeoxyglucose. Radiol. Clin. 42 (6), 1033–1053.
Smith, Timothy Andrew Davies, 1999. Facilitative glucose transporter expression in human cancer tissue. Br. J. Biomed. Sci. 56 (4), 285.
Smith, Timothy Andrew Davies, 2000. Mammalian hexokinases and their abnormal expression in cancer. Br. J. Biomed. Sci. 57 (2), 170.
Sousa, Sergio Filipe, Fernandes, Pedro Alexandrino, Ramos, Maria Joao, 2006. Protein–ligand docking: current status and future challenges. Proteins: Struct., Funct., Bioinf. 65 (1), 15–26.
Tekin, H.O., Akman, F., Issa, Shams A.M., Kaçal, M.R., Kilicoglu, O., Polat, H., 2020. Two-step investigation on fabrication and characterization of iron-reinforced novel composite materials for nuclear-radiation shielding applications. J. Phys. Chem. Solid. 146 (November), 109604 https://doi.org/10.1016/j.jpcs.2020.109604.
Vahapoglu, Beyza, Kilicoglu, Ozge, Nur, Cebi, Ayseli, Mehmet Turan, Kara, Umit, Sagdic, Osman, Capanoglu, Esra, 2022. Investigating the effect of gamma-ray interaction on the stability and physicochemical properties of turmeric and ginger using Monte Carlo simulation. Radiat. Phys. Chem. 201, 110413.
Vermeulen, Koen, Vandamme, Mathilde, Guy, Bormans, Cleeren, Frederik, 2019. Design and challenges of radiopharmaceuticals. In: Seminars in Nuclear Medicine, vol. 49. Elsevier, pp. 339–356.
Ziegler, J., Biersack, J., Ziegler, M., 2008. SRIM, the Stopping and Range of Ions in Matter. SRIM Company. *URL* Https://Books. Google. Com/Books.
Ziegler, James F., 2004. SRIM-2003. Nucl. Instrum. Methods Phys. Res. Sect. B Beam Interact. Mater. Atoms 219, 1027–1036.